International Journal of Electrical, Electronic and Communication Sciences
ISSN: 2517-9438
Vol:3, No:1, 2009

Implementation of an On-Line PD Measurement System Using HFCT

F. Haghjoo, M. Sarlak and S.M. Shahrtash

***Abstract*—**In order to perform on-line measuring and detection of PD signals, a total solution composing of an HFCT, A/D converter and a complete software package is proposed. The software package includes compensation of HFCT contribution, filtering and noise reduction using wavelet transform and soft calibration routines. The results have shown good performance and high accuracy.

***Keywords*—**Partial Discharge, Measurement, On-line, HFCT

I. Introduction

MV and HV power cables represent a large role in electrical networks. Insulation failure in them can lead to costly interruption of supply, and therefore, continuous supervising their insulation quality is a necessary need. The earlier detection of insulation degradation can prepare easier substitution or renovation before failure.

Partial discharge (PD) measurement can be used as a diagnostic method for detecting degradation and for avoiding of insulation breakdown. The damage due to PD can be estimated depending on the type of discharge; for example, internal or surface discharge, termination discharge, corona, and electrical treeing [1].

For XLPE cables, internal PD activity is regarded as the most dangerous because of progressive deterioration due to internal PDs develops very quickly to ultimate failure.

On-line PD monitoring is the most effective technique for insulation assessment with two advantages:

- No need to supply interruption
- Availability of continuous assessment of insulation degradation (if exists) and its trend

However, it has some major difficulties, such as:

1. Very low level PD signals against very high level noises in nominal voltage (electromagnetic interference and other environmental noises)
2. Distortion of PD signals when they are picked up by the sensors
3. On-line calibration

Conventionally, the main techniques used to reduce noises in PD signals have been realized in either the time domain or in the frequency domain. The Wavelet Transform (WT) technique provides a new noise reduction tool which provides the transformed components in both the time and frequency domains. Using automated thresholding [2], the noises can be rejected from PD signals. Also, by zeroing some WT detail components, the initial signals can be filtered as narrowband or broadband, arbitrarily.

Any sensor used as a transfer medium for PD signals, has its own transfer function which alters the original signal in the output. High frequency current transformers (HFCTs) are one type of these sensors which eliminates the low frequencies and passes the mid and high frequencies according to their frequency response characteristics. This alternation must be considered in PD reconstruction and status of insulation degradation.

Another complexity is the calibration of measuring and detection system in on-line applications. Environmental and electromagnetic noises have variable magnitudes and frequencies. Therefore, there is a need to use an algorithm for on-line adjustment of the measuring system.

Implementation of a comprehensive system for On-Line PD detection and measurement, with a total solution for the above-mentioned complexities, has been described in this paper. The designed system includes HFCT as detector, A/D converter and different numerical algorithms for correction of HFCT characteristic, applying wavelet based signal decomposition, providing adaptive thresholding and noise reduction, reconstruction of the PD signals based on arbitrary frequency band (narrow or broadband) and finally showing PD parameters and patterns.

F. Haghjoo is PhD candidate of Department of Electrical Engineering, Iran University of Science and Technology, Narmak, Tehran, Iran (email: farhadhaghjoo@gmail.com).

M. Sarlak is PhD candidate of Department of Electrical Engineering, Iran University of Science and Technology, Narmak, Tehran, Iran (email: sarlak@iust.ac.ir).

S. M. Shahrtash is with the "Center of Excellence for Power System Automation and Operation (CEPSAO)" associated to Iran University of Science and Technology, Narmak, Tehran, Iran (corresponding author to provide phone: +98 21 77240490; fax: +98 21 77240494; e-mail: shahrtash@iust.ac.ir).

The major features of this system are:

1. Performing data acquisition by using clamp HFCT, so there is no need to HV connections;
2. Correction and modification of obtained distorted signal from HFCT, and therefore, compensated data acquisition operation is done;
3. No need to power outage of the test object;
4. Selectable frequency band for the measurement;
5. Adaptive determination of the threshold values in noise reduction procedure;
6. Capability to operate in two modes:
   - with applying on-line calibration signal to the hardware
   - with off-line calibration (stored files are used in this case)
7. High immunity for the operator.

II. Proposed Detection System

The proposed system is schematically shown in Fig.1, where the PD signals are obtained by HFCT, converted to digital samples by A/D converters and applied to the proposed signal processing algorithm.

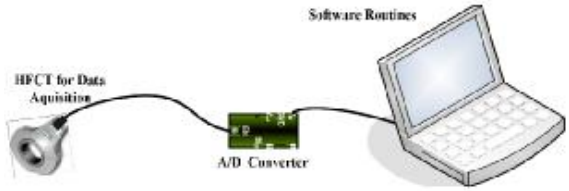

Fig.1 Schematic of the designed system

The main parts of the algorithm and their arrangement are shown in Fig.2, where each part has been described in the following sections.

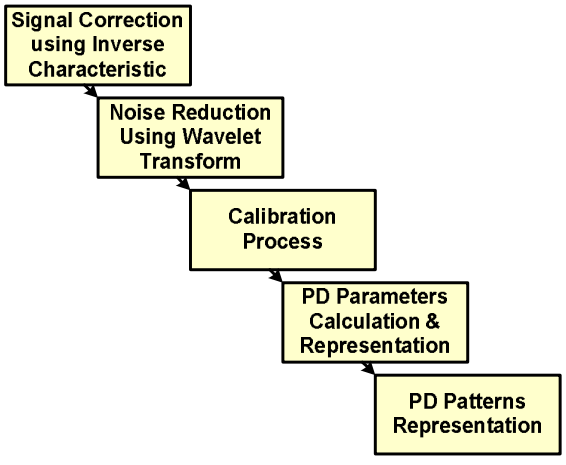

Fig.2 The hierarchy of the proposed system

III. Compensation of HFCT Effect

Fig.3 shows the schematic diagram of an HFCT feeding a resistive burden (standing for the input impedance of A/D converter) and its equivalent circuit, where r and L are the coil resistance and leakage inductance, respectively, C is the total stray capacitance of the coil (to be considered in high frequencies) and R is the resistive burden. According to the current passing through the primary circuit, i_p, the induced voltage on the coil is equal to:

$$e_{coil} = -M\frac{di_p}{dt} \quad (1)$$

where $M = n\mu A_c / \ell_c$, and n, μ, A_c and ℓ_c are number of coil turns, core permeability, core cross section and core length, respectively.

Then the transfer function of V_{out} can be deduced as:

$$V_{out}(s) = \frac{-sRM}{s^2RLC + s(L+RC) + (R+r)} I_p(s) \quad (2)$$

where the magnitude and phase angle of its frequency response are shown in Fig.4.

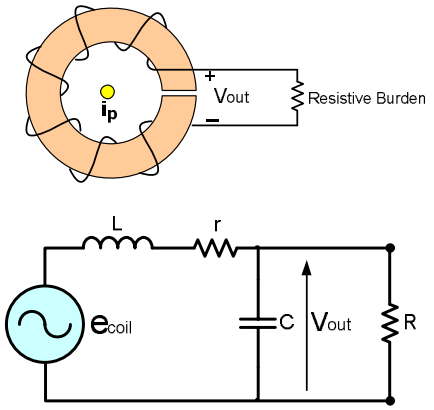

Fig.3 Schematic diagram of an HFCT feeding a resistive burden (top) and its equivalent circuit (down)

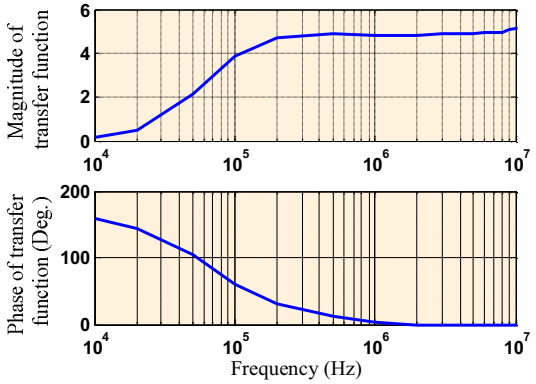

Fig.4 Magnitude (top) and Phase angle (down) of the HFCT transfer function

But the procedure is vice versa, i.e. it is the frequency response of HFCT which is available, through measuring, and the transfer function must be drawn. This transfer function derivation is performed through a fitting algorithm by introducing the unknown output transfer function as:

$$H(s)=\frac{a_2 s^2+a_1 s+a_0}{s^2+b_1 s+b_0} \tag{3}$$

and deriving

$$G\cdot X=-Y \tag{4}$$

where $X=[a_0 \quad a_1 \quad a_2 \quad b_0 \quad b_1]^T$ and

$$G=\begin{bmatrix} \frac{1}{\omega_1^2} & 0 & -1 & -\frac{\mathrm{Re}\{H(j\omega_1)\}}{\omega_1^2} & \frac{\mathrm{Im}\{H(j\omega_1)\}}{\omega_1} \\ 0 & \frac{1}{\omega_1} & 0 & -\frac{\mathrm{Im}\{H(j\omega_1)\}}{\omega_1^2} & \frac{\mathrm{Re}\{H(j\omega_1)\}}{\omega_1} \\ \frac{1}{\omega_2^2} & 0 & -1 & -\frac{\mathrm{Re}\{H(j\omega_2)\}}{\omega_2^2} & \frac{\mathrm{Im}\{H(j\omega_2)\}}{\omega_2} \\ 0 & \frac{1}{\omega_2} & 0 & -\frac{\mathrm{Im}\{H(j\omega_2)\}}{\omega_2^2} & \frac{\mathrm{Re}\{H(j\omega_2)\}}{\omega_2} \\ \vdots & \vdots & \vdots & \vdots & \vdots \\ \frac{1}{\omega_N^2} & 0 & -1 & -\frac{\mathrm{Re}\{H(j\omega_N)\}}{\omega_N^2} & \frac{\mathrm{Im}\{H(j\omega_N)\}}{\omega_N} \\ 0 & \frac{1}{\omega_N} & 0 & -\frac{\mathrm{Im}\{H(j\omega_N)\}}{\omega_N^2} & \frac{\mathrm{Re}\{H(j\omega_N)\}}{\omega_N} \end{bmatrix} \tag{5}$$

$$Y=\begin{bmatrix} \mathrm{Re}\{H(j\omega_1)\} \\ \mathrm{Im}\{H(j\omega_1)\} \\ \mathrm{Re}\{H(j\omega_2)\} \\ \mathrm{Im}\{H(j\omega_2)\} \\ \vdots \\ \vdots \end{bmatrix} \tag{6}$$

and ω_1, ω_2 ,…, ω_n are the frequencies at which the frequency response of the output transfer function has been measured.

Then using least square error technique, the best estimation of the coefficients has been found as:

$$X=-\left(G^T G\right)^{-1} G^T Y \tag{7}$$

Performing the above process, i.e. measuring the frequency response, fitting the transfer function and estimating the coefficients, it is possible that one zero on the RHS of the complex plane that will appear as an unstable pole in $H^{-1}(s)$.

With neglecting the fitting process in low frequencies (due to the elimination of those frequencies by applying Wavelet Transform to the outputs of the procedure of HFCT correction and being approved by [3] that for PD measurements the required frequency bandwidth is from 30-70 up to some hundred kHz), the problem of RHS zero is solved (although the fitting error is increased in low frequencies, which are eliminated later).

The available HFCT in the prototype system gives a_0=15848778026.35, a_1=48248.45, a_2=4.86, b_0=157709798462.13, and b_1=664667.41 through the latter method. The frequency response of the fitted transfer function (according to the data limited to 50 kHz-10 MHz) is shown in Fig.5.

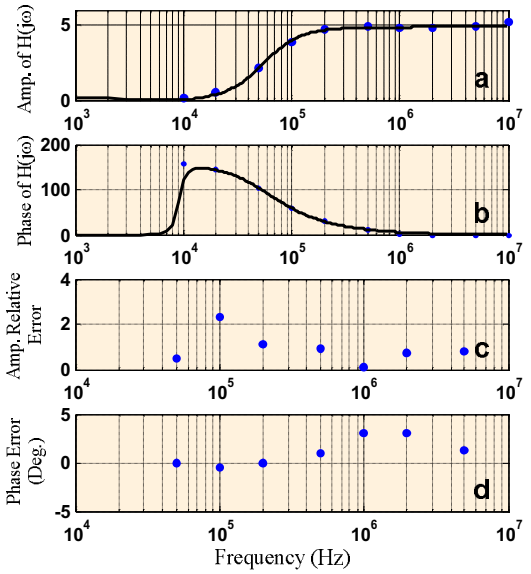

Fig.5 a) Amplitude of HFCT transfer function
b) Phase of HFCT transfer function
c) Amplitude relative error
d) Phase error

Now in order to compensate the effect of the sensor (HFCT in this system) on the original PD signals the inverse of the HFCT transfer function must be applied to the HFCT output. To perform this calculation, first, H(s) is converted to H(z) in z-domain, where it can be easily derived as:

$$H(z)=\frac{K_2 z^{-2}+K_1 z^{-1}+K_0}{J_2 z^{-2}+J_1 z^{-1}+J_0} \tag{8}$$

where:

$$\begin{cases} K_2=a_2(2/T_s)^2-a_1(2/T_s)+a_0 \\ K_1=2(a_0-a_2(2/T_s)^2) \\ K_0=a_2(2/T_s)^2+a_1(2/T_s)+a_0 \\ J_2=b_2(2/T_s)^2-b_1(2/T_s)+b_0 \\ J_1=2(b_0-b_2(2/T_s)^2) \\ J_0=b_2(2/T_s)^2+b_1(2/T_s)+b_0 \end{cases} \tag{9}$$

and T_s is the sampling period. Then the compensated current (PD signals) is obtained, in time-domain, as:

$$i_{in}^{cal}(k)=\frac{J_0}{K_0}v_{out}^{sen}(k)+\frac{J_1}{K_0}v_{out}^{sen}(k-1)+\frac{J_2}{K_0}v_{out}^{sen}(k-2)-\frac{K_1}{K_0}i_{in}^{cal}(k-1)-\frac{K_2}{K_0}i_{in}^{cal}(k-2) \quad (10)$$

The final result of the above compensation method is shown in Fig.6 where the good performance can be deduced by comparing the final and original signals and/or the depicted relative error.

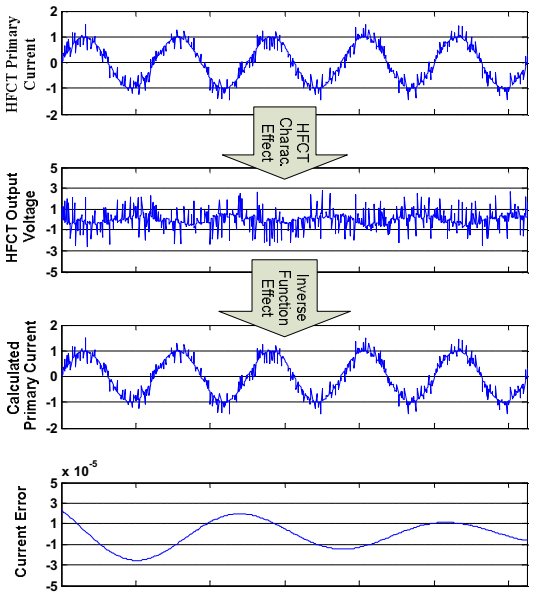

Fig.6 Effect of HFCT transfer function and its inverse

IV. Filtering Using WT

Filtering of obtained signals can be done easily using WT. Based on this transformation, any sampled signal can be divided to several details and one approximate component that any of them includes a pre-defined frequency bandwidths. These bandwidths depend on the sampling frequency (f_s), where if it is considered as 10 MS/sec, the first detail d_1 is the filtered input signal in 2.5 to 5 MHz frequency band. Also, the second one d_2 gives the input signal in frequency range of 1.25 to 2.5 MHz and so on. If there are k detail components, the k^{th} detail component includes the frequency range of $f_s/2^{k+1}$ up to $f_s/2^k$ and the k^{th} approximate component includes any component with frequency less than $f_s/2^{k+1}$. These properties of details and approximate component are shown in Fig.7 for three levels of decomposition.

Fig.8 shows the reconstruction process for three detail and the last approximate components. R, as reconstruction matrix [4], is created according to G and H elements. This matrix generates the elements of the previous ($(k-1)^{th}$) approximate component using the elements of detail and approximate components of any (k^{th}) level, sequentially.

Zeroing the last approximate component means that the low frequency band is eliminated. Also, zeroing of any detail is equal to the elimination of the relevant frequency band. Therefore, any of the above details represents a specified filtered component, of course after reconstruction process.

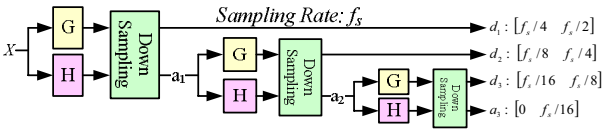

Fig.7 Three levels decomposition using WT and their frequency bands

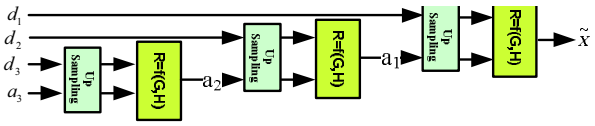

Fig.8 Three levels reconstruction using details and approximate components

Using 10 MS/sec as sampling frequency, the seventh approximate component including low frequency components (less than about 39 kHz) can be eliminated for PD measurements. Also, not only the first detail, but also any of the second, third and even fourth detail component can be eliminated, arbitrarily. For example, by elimination of the two first details and seventh approximate components, reconstruction process will be done in 39 kHz up to 1.25 MHz frequency band, as a broadband PD measurement. Also, by elimination of the approximate and all of details components except the fourth detail component, the narrow band measurement can be done for 312 up to 625 kHz.

The proposed system accepts adjustable sampling frequency up to 10 MHz and then the maximum number of decomposition level is determined, providing that the last approximate component includes the frequency components of less than 40 kHz. By default, the first detail and the last approximate components are eliminated by the system.

V. Automatic Noise Reduction Using WT

Well-known method for noise reduction on the basis of WT components is the method of automatic thresholding for any detail component [2].

In this method and after decomposition process, threshold

values for all detail components are calculated by:

$$\lambda_k = (m_k / 0.6745).\sqrt{2.\log(n_k)} \quad (11)$$

where m_k is the median and n_k is the number of the k^{th} detail elements.

Then, all of elements at any level can be modified using '*Soft'* or *'Hard'* thresholding method. In both methods, any element that has smaller (absolute) value than the threshold will be zeroed. In the hard method any other element will be remained without any change, but in the soft one they will be shifted toward zero by the same amount as the threshold value.

In some cases, the number and magnitude of PD signals may be larger in comparison with the ambient noises. In such conditions, m_ks will be calculated mostly according to PD signals instead of the noises, which can decrease the measurement accuracy.

For solving the above problem, it is possible to modify m_ks after initial calculation through the following procedure:

1. Determination of λ_k for any detail component based on n_k elements
2. Elimination of any element that has an absolute value larger than λ_k from n_k elements and also reduction of n_k (i.e. the number of detail elements participating in calculation of m_ks)
3. Determination of λ_k^{mod}, based on the reduced set of detail elements.

As, in the last step, there is not any element with larger value than the λ_k, therefore it can be deduced that $\lambda_k^{\text{mod}} < \lambda_k$, and although their difference may be high for laboratorial tests (shielded locations), it can approach to zero for on-site/on-line tests.

By using this process some small noises may appear in the output, but the accuracy is increased. On the other hand, small noises and/or very little PD pulses, appeared in the output signal, can be eliminated using another threshold value (for example, 10% of the biggest PD magnitude).

Anyway, to increase the measuring accuracy, threshold values must be modified and more modification steps give more accuracy to the PD measurement, but it will consume more time. Although, by experience, one modification is enough, the designed software system is adjusted for three times modification.

VI. System Calibration

PD measuring systems should be re-calibrated while either test conditions or test object changes.

In the commercial PD measuring systems, the magnitude of PD pulses, passing through the capacitive sensors, are considered as apparent charge values. The magnitude of these pulses is compared to the electrical charge of pulses of calibration signals that are generated with an R-C circuit. This ratio determines the calibrating factor (k_c).

The designed system is able to save calibration signals of different pico-coulombs, obtained in low noise conditions (e.g. at shielded test rooms) and, then, to use them in on-site/on-line conditions. Therefore, the proposed measuring system dose not need to be calibrated through applying the calibration signal across the hardware, and the calibration process can be performed through the software, by applying the signal from its library.

For suitable system calibration, the same process, performed for the sampled signals, should be done for the calibration signals. Therefore, calibration signals must be decomposed, and after thresholding (but with the same λ_k s as for the original signal), reconstructed, in similar procedure as above-mentioned. Finally, k_c can be determined according to any of the following methods:

1. Commercial procedure:

In this method k_c will be determined as:

$$k_c^{comm} = \frac{q_{Cal}^{ini}}{A_{Cal}^{rec}} \quad (12\text{-}1)$$

while q_{Cal}^{ini} is the electrical charge of initially calibration signal and A_{Cal}^{rec} is amplitude of reconstructed calibrating signal.

2. Amplitude based procedure:

In this method k_c will be determined as:

$$k_c^{amp} = \frac{A_{Cal}^{ini}}{A_{Cal}^{rec}} \quad (12\text{-}2)$$

while A_{Cal}^{ini} and A_{Cal}^{rec} are the amplitudes of the initially calibration signal and the reconstructed calibrating signal, respectively.

3. Integral based procedure:

In this method k_c will be determined as:

$$k_c^{\text{int}} = \frac{q_{Cal}^{ini}}{q_{Cal}^{rec}} \quad (12\text{-}3)$$

while q_{Cal}^{ini} and q_{Cal}^{rec} are the electrical charges (integral of current pulses) of the initially calibration signal and the reconstructed calibrating signal, respectively.

VII. Output PD Parameters and Patterns

PD measuring systems should be re-calibrated while either test conditions or test object changes.

Any PD measuring system should be able to represent PD parameters. Designed system can represent not only PD integration parameters, but also some of the parameters of PD patterns, based on [3]. These are listed as below:

1. Apparent charge of any of individual PD current pulses (q_i) during a pre-defined time (T_{ref}).
2. Width of any individual PD current pulses.
3. Peak of any individual PD current pulses.
4. Maximum magnitude of PD pulses (or apparent charges) in a pre-defined time.
5. PD Repetition Rate (N) during a pre-defined time.
6. Average Discharge Current (I_{pd}) during a pre-defined time as:

$$I_{PD} = \frac{1}{T_{ref}} \sum_i |q_i| \quad (13)$$

7. PD Quadratic Rate (D) as:

$$D = \frac{1}{T_{ref}} \sum_i q_i^2 \quad (14)$$

8. Distribution of the number of PD pulses versus to their width.
9. Distribution of the number of PD pulses versus to their peaks.
10. Distribution of the number of PD pulses versus to their apparent charges.

VIII. Implementation and Outputs

The above-mentioned four numerical procedures, as depicted in Fig.2, with all the possible options for the operation were implemented in a PC-based system, where the input signals were drawn through the route of HFCT and A/D converter (as shown in Fig.1).

Fig.9 shows the original high noisy signal and the cleaned (de-noised) reconstructed output signal after calibration by commercial procedure, where some PD signals have been detected, by applying low sensitivity threshold to the output, i.e. the output samples with smaller magnitudes than 0.3 of the largest one are eliminated. There are, also, some large pulses in the input signal (marked as 2 in Fig.9), which were expected to appear as PD pulses in the output signal; but it does not, according to the accurate performance of the proposed system. Enlarging the input signal around that point, as shown in Fig.10, approves that it is not a PD pulse and is really a noise. Also, investigating the details of the original signal around the point marked by 1 in Fig.9 shows the good performance of the proposed system in detecting PD pulses and depicting in output signal (Fig.11).

Other parameters of the PD pulses of the original signal (defined in the previous section) are given in Table1 which are calculated after signal reconstruction.

TABLE1
Typical PD Parameters of an Obtained Signal

Parameter	Value
$q_{average}$	323 pC
q_{max}	2080 pC
N	2650 pulses/sec
I_{PD}	848 nA
D	745 $(nC)^2$/sec

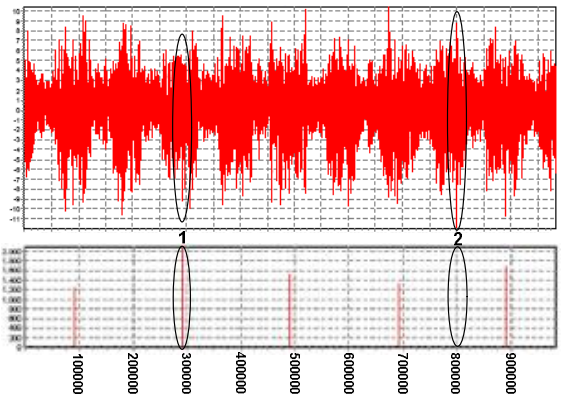

Fig.9 Input (top) and output signal after noise reduction and calibration (down) with low sensitivity mode

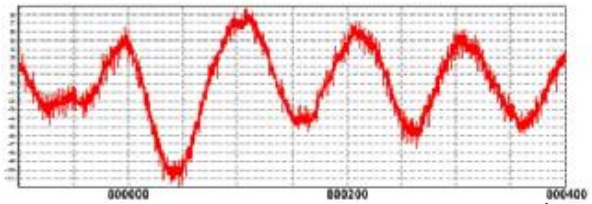

Fig.10 Magnifying of the input signal around 800000th sample. This peak is considered as noise by designed system.

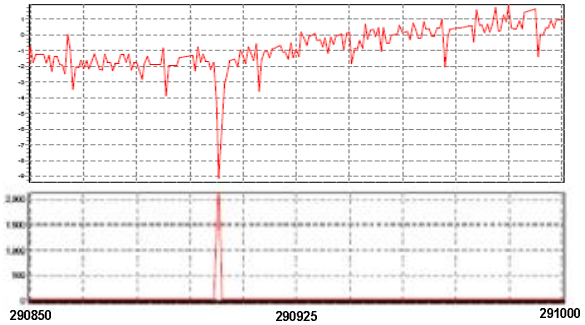

Fig.11 Magnifying of input and output signals around 290000th sample. This peak is considered as PD by designed system.

IX. Conclusion

In this paper a total solution for on-line measuring, detection and signal processing of PD signals has been proposed. The whole system including HFCT and A/D converter and the software algorithms developed on a personal computer has been implemented. Also the four main algorithms have been described, which are:

1. Compensation of the frequency characteristic of HFCT (as the input sensor),
2. Narrow and/or Broad band Filtering using wavelet transform
3. Noise reduction using automatic and modified threshold calculation,
4. Soft calibration (without the need to hardware devices).

Results show the good performance of the proposed system.

References

[1] I. Shim, J.J. Soraghan, and W. H.Siew, "A noise reduction techniques for on-line detection and location of partial discharges in high voltage cable networks", IEE Meas. Sci. Technol., Vol. 11, pp. 1708-1713, 2000.
[2] X.Ma, C.Zhou, I.J.Kemp, "Automated Wavelet Selection and Thresholding for PD Detection", IEEE Electrical Insulation Magazine, Vol. 18, No. 2, pp. 37-45, 2002.
[3] IEC 60270-2000, "High voltage test techniques-partial discharge measurements".
[4] S. Mallat, A Wavelet Tour of Signal Processing, Second Edition, Academic Press: California, pp. 255-256, 1999.